Effects of variable chemical reaction and variable electric conductivity on free convective heat and mass transfer flow along an inclined stretching sheet with variable heat and mass fluxes under the influence of Dufour and Soret effects

M.S. Alam, M.U. Ahammad

Department of Mathematics
Dhaka University of Engineering and Technology (DUET)
Gazipur-1700, Bangladesh
msalam631@yahoo.com

Abstract. This paper deals with the effects of variable chemical reaction and variable electric conductivity on free convection and mass transfer flow of a viscous, incompressible and electrically conducting fluid over an inclined stretching sheet with variable heat and mass fluxes under the influence of Dufour and Soret effects. The non-linear boundary layer equations with boundary conditions are transferred into a system of non-linear ordinary differential equations using an established similarity transformation. These non-linear and locally-similar ordinary differential equations are solved numerically by applying Nachtsheim–Swigert shooting iteration technique with sixth-order Runge–Kutta integration scheme. Comparison with previously published work is obtained and excellent agreement is found. The effects of various parameters on the dimensionless velocity, temperature and concentration profiles as well as the local skin-friction coefficient, heat and mass transfer rate from the stretching sheet to the surrounding fluid are presented graphically and in tabulated form for a hydrogen-air mixture. The numerical results showed that chemical reaction parameter K, order of reaction n, Dufour number Df, Soret number Sr and heat (or mass) flux parameter r play a crucial role in the solutions.

Keywords: heat and mass transfer, chemical reaction, variable electric conductivity, stretching sheet, Dufour effect, Soret effect.

1 Introduction

Coupled heat and mass transfer problems in presence of chemical reaction are of importance in many processes and thus have received considerable amount of attention in recent times. In processes such as drying, distribution of temperature and moisture over agricultural fields and groves of fruit trees, damage of crops due to freezing, evaporation at the surface of a water body, energy transfer in a wet cooling tower and flow in a desert

cooler, heat and mass transfer occur simultaneously. Many practical diffusive operations involve the molecular diffusion of a species in the presence of chemical reaction within or at the boundary. Therefore, the study of heat and mass transfer with chemical reaction is of great practical importance to engineers and scientists. Andersson et al. [1] studied the diffusion of a chemically reactive species from a stretching sheet. Anjalidevi and Kandasamy [2] investigated the effects of chemical reaction and heat and mass transfer on a laminar flow along a semi-infinite horizontal plate. Flow and mass transfer on a stretching sheet with a magnetic field and chemically reactive species have been investigated by Takhar et al. [3]. Afify [4] analyzed the MHD free convective flow and mass transfer over a stretching sheet with homogeneous chemical reaction of order n (where n was taken $1, 2$ and 3) and with a constant rate. Abo-Eldahab and Salem [5] studied MHD flow and heat transfer of non-Newtonian power-law fluid with diffusion and chemical reaction on a moving cylinder. The order of the chemical reaction in that paper was taken as $n = 1, 2$ and 3. Alam et al. [6] investigated the effects of first order chemical reaction and thermophoresis on MHD mixed convective heat and mass transfer flow along an inclined plate in the presence of heat generation/absorption with viscous dissipation and joule heating. Recently, Alam et al. [7] investigated the effects of variable chemical reaction (where n was taken $1, 2$ and 3), thermophoresis, temperature dependent viscosity and thermal radiation on an unsteady MHD free convective heat and mass transfer flow past in impulsively started infinite inclined porous plate.

But in the above mentioned studies, Dufour and Soret terms have been neglected from the energy and concentration equations respectively. It has been found that energy flux can be generated not only by temperature gradient but also by concentration gradient as well. The energy flux caused by concentration gradient is called Dufour effect and the same by temperature gradient is called the Soret effect. These effects are very significant when the temperature and concentration gradient are very high. The importance of these effects in convective transport in clear fluids has been studied by Bergaman and Srinivasan [8] and Zimmerman et al. [9]. Kafoussias and Williams [10] studied thermal-diffusion and diffusion-thermo effects on mixed free-forced convective and mass transfer boundary layer flow with temperature dependent viscosity. Anghel et al. [11] studied the Dufour and Soret effects on free convection boundary layer over a vertical surface embedded in a porous medium. Postelnicu [12] analyzed the influence of magnetic field on heat and mass transfer from vertical surfaces in porous media considering Soret and Dufour effects. Alam et al. [13] investigated the Dufour and Soret effects on steady MHD combined free-forced convective and mass transfer flow past a semi-infinite vertical plate. Chamkha and Ben-Nakhi [14] analyzed MHD mixed convection-radiation interaction along a permeable surface immersed in a porous medium in the presence of Soret and Dufour's effects. El-Aziz [15] studied thermal-diffusion and diffusion-thermo effects on combined heat and mass transfer by hydromagnetic three-dimensional free convection over a permeable stretching surface with radiation. Afify [16] obtained similarity solution for the effects of thermal diffusion and diffusion thermo on MHD free convective heat and mass transfer over a stretching surface considering suction or injection. His numerical results indicate that for fluids with medium molecular weight (H_2, air), Dufour and Soret effects should not be neglected and the suction as well as injection parameter has significant impact

in controlling the rate of heat transfer in the boundary layer. Anwar Bég et al. [17] studied numerically free convection magnetohydrodynamic heat and mass transfer from a stretching surface to a saturated porous medium with Soret and Dufour effects. Very recently, Hayat et al. [18] analyzed heat and mass transfer for Soret and Dufour's effect on mixed convection boundary layer flow over a stretching vertical surface in a porous medium filled with a viscoelastic fluid.

Therefore our aim of the present paper is to investigate the effects of variable chemical reaction and variable electric conductivity on free convective flow with heat and mass transfer over an inclined permeable stretching sheet under the influence of Dufour and Soret effects with variable heat and mass fluxes. It should be mentioned here that the reaction having order four or more are practically impossible. Therefore unlike the works of Afify [4] and Abo-Eldahab and Salem [5] we have also taken the order of the reaction as $n = 1, 2$ and 3 in this paper.

2 Governing equations of the flow and similarity analysis

Let us consider a steady two-dimensional; laminar MHD free convective heat and mass transfer flow of a viscous and incompressible fluid along a linearly stretching semi-infinite sheet that is inclined from the vertical with an acute angle α. The surface is assumed to be permeable and moving with velocity, $u_w(x) = bx$ (where b is constant called stretching rate). Fluid suction is imposed at the stretching surface. The x-axis runs along the stretching surface in the direction of motion with the slot as the origin and the y-axis is measured normally from the sheet to the fluid. The applied magnetic field is primarily in the y-direction and varies in strength as a function of x and is defined as $\mathbf{B} = (0, B(x))$. Moreover, the electrical conductivity σ is assumed to have the form as $\sigma = \sigma_0 u$, where σ_0 is a constant. We further assume that there exists a homogeneous chemical reaction between the fluid and species concentration.

Under the above assumption and along with Boussinesq's approximation, the governing equations describing the conservation of mass, momentum, energy and concentration respectively are as follows:

$$\frac{\partial u}{\partial x} + \frac{\partial v}{\partial y} = 0, \tag{1}$$

$$u\frac{\partial u}{\partial x} + v\frac{\partial u}{\partial y} = \nu\frac{\partial^2 u}{\partial y^2} + g\beta(T-T_\infty)\cos\alpha + g\beta^*(C-C_\infty)\cos\alpha - \frac{\sigma(B(x))^2}{\rho}u, \tag{2}$$

$$u\frac{\partial T}{\partial x} + v\frac{\partial T}{\partial y} = \frac{k}{\rho c_p}\frac{\partial^2 T}{\partial y^2} + \frac{D_m k_T}{c_s c_p}\frac{\partial^2 C}{\partial y^2}, \tag{3}$$

$$u\frac{\partial C}{\partial x} + v\frac{\partial C}{\partial y} = D_m\frac{\partial^2 C}{\partial y^2} + \frac{D_m k_T}{T_m}\frac{\partial^2 T}{\partial y^2} - K_l(C-C_\infty)^n, \tag{4}$$

where u, v are the velocity components in the x and y directions respectively, ν is the kinematic viscosity, g is the acceleration due to gravity, ρ is the density of the fluid, β is the volumetric coefficient of thermal expansion, β^* is the volumetric coefficient of

expansion with concentration, T and T_∞ are the temperature of the fluid inside the thermal boundary layer and the fluid temperature in the free stream, respectively, while C and C_∞ are the corresponding concentrations, k is the thermal conductivity of fluid, c_s is the concentration susceptibility, c_p is the specific heat at constant pressure, D_m is the molecular diffusivity of the species concentration, T_m is the mean fluid temperature, k_T is the thermal diffusion ratio, K_l is the reaction rate and n is the order of chemical reaction.

For the flow under study, it is relevant to assume that the applied magnetic field strength $B(x)$ has the form (see also Helmy [19]):

$$B(x) = \frac{B_0}{\sqrt{x}}, \quad B_0 \text{ is constant.} \tag{5}$$

The fourth term in equation (2), taking into account equation (5) can be rewritten as:

$$\frac{\sigma(B(x))^2 u}{\rho} = \frac{\sigma_0 B_0^2 u^2}{\rho x}, \quad \text{where } \sigma = \sigma_0 u. \tag{6}$$

Therefore using equation (6) into equation (2), the momentum equation can be rewritten as:

$$u\frac{\partial u}{\partial x} + v\frac{\partial u}{\partial y}$$
$$= \nu\frac{\partial^2 u}{\partial y^2} + g\beta(T - T_\infty)\cos\alpha + g\beta^*(C - C_\infty)\cos\alpha - \frac{\sigma_0 B_0^2}{\rho x}u^2. \tag{7}$$

The appropriate boundary conditions are given by:

$$u = u_w(x) = bx, \quad v = \pm v_w(x),$$
$$-k\frac{\partial T}{\partial y} = q_w = A_1 x^r, \quad -D_m\frac{\partial C}{\partial y} = M_w = A_2 x^r \quad \text{at } y = 0, \tag{8a}$$
$$u = 0, \quad T = T_\infty, \quad C = C_\infty \quad \text{as } y \to \infty, \tag{8b}$$

where b is a constant called stretching rate and A_1, A_2 are proportionality constants and $v_w(x)$ represents the permeability of the porous surface where its sign indicates suction (< 0) or injection (> 0). Here r is the heat (or mass) flux exponent parameter. For $r = 0$, the accelerating sheet is subject to uniform heat (or mass) flux.

Now following Acharya et al. [20], let us consider the similarity variable as:

$$u = \frac{\partial\psi}{\partial y}, \quad v = -\frac{\partial\psi}{\partial x}$$
$$\psi = (\nu b)^{1/2} x f(\eta), \quad \eta = (b/\nu)^{1/2} y,$$
$$T - T_\infty = \frac{A_1 x^r}{k}(\nu/b)^{1/2}\theta(\eta), \tag{9}$$
$$C - C_\infty = \frac{A_2 x^r}{D_m}(\nu/b)^{1/2}\phi(\eta).$$

Thus equations (7), (3) and (4) respectively become

$$f''' + ff'' - (f')^2 + g_s\theta\cos\alpha + g_c\phi\cos\alpha - M(f')^2 = 0, \tag{10}$$

$$\theta'' - rPrf'\theta + Prf\theta' + PrDf\phi'' = 0, \tag{11}$$

$$\phi'' - rScf'\phi + Scf\phi' + ScSr\theta'' - ScK\phi^n = 0. \tag{12}$$

The boundary conditions (8) then turn into

$$f = f_w, \quad f' = 1, \quad \theta' = -1, \quad \phi' = -1 \quad \text{at } \eta = 0, \tag{13a}$$

$$f' = 0, \quad \theta = 0, \quad \phi = 0 \quad \text{as } \eta \to \infty, \tag{13b}$$

where $f_w = -v_w/(b\nu)^{1/2}$is the dimensionless wall mass transfer coefficient such that $f_w > 0$ indicates wall suction and $f_w < 0$ indicates wall injection.

The dimensionless parameters introduced in the above equations are defined as follows:

$M = \sigma B_0^2 x/\rho u_w(x)$ is the local magnetic field parameter,

$Gr = g\beta q_w x^4/k\nu^2$ is the local Grashof number,

$Gm = g\beta^* M_w x^4/D_m\nu^2$ is the local modified Grashof number,

$Re_x = u_w(x)x/\nu$ is the local Reynolds number,

$g_s = Gr/Re_x^{5/2}$ is the temperature buoyancy parameter,

$g_c = Gm/Re_x^{5/2}$ is the mass buoyancy parameter,

$Df = D_m M_w k_T/\nu c_s c_p q_w$ is the Dufour number,

$Sr = D_m q_w k_T/k M_w T_m$ is the Soret number,

$Pr = \nu\rho C_p/k$ is the Prandtl number,

$Sc = \nu/D_m$ is the Schmidt number and

$K = K_l(C_w - C_\infty)^{n-1}x/u_w(x)$ is the local chemical reaction parameter.

The parameters of engineering interest for the present problem are the local skin-friction coefficient, local Nusselt number and the local Sherwood number which are obtained from the following expressions:

$$\frac{1}{2}Cf_x(Re_x)^{\frac{1}{2}} = f''(0), \tag{14}$$

$$Nu_x(Re_x)^{-\frac{1}{2}} = \frac{1}{\theta(0)}, \tag{15}$$

$$Sh_x(Re_x)^{-\frac{1}{2}} = \frac{1}{\phi(0)}. \tag{16}$$

3 Numerical solution

The system of transformed nonlinear ordinary differential equations (10)–(12) together with boundary condition (13) have been solved numerically by utilizing a modification of the program suggested by Nachtsheim–Swigert [21] shooting iteration technique with

sixth-order Runge–Kutta integration scheme (for detailed discussion of this method see also Alam et al. [22]). Various groups of the parameters g_s, g_c, f_w, Pr, Sc, Df, Sr, K, n, M and α were considered in different phases. In all the computations the step size $\Delta\eta = 0.01$ was selected that satisfied a convergence criterion of 10^{-6} in almost all of different phases mentioned above. The value of η_∞ was found to each iteration loop by the statement $\eta_\infty = \eta_\infty + \Delta\eta$. The maximum value of η_∞ for each group of parameters has been obtained when the value of the unknown boundary conditions at $\eta = 0$ does not change in the successful loop with an error less than 10^{-6}.

To assess the accuracy of the present numerical method, we have compared our rate of heat transfer $(1/\theta(0))$ with those of Elbashbeshy [23] and Chen [24] for their Newtonian fluid case in the absence of magnetic field in Table 1 and we found that excellent agreement among the results exists. Therefore, the developed code can be used with great confidence to study the problem considered in this paper.

Table 1. Comparison of $(1/\theta(0))$ with Elbashbeshy [23] and Chen [24] for their Newtonian fluid case and for our $\alpha = 90°$, $f_w = 0.6$, $Sc = 0.22$ and $M = g_s = g_c = K = r = Sr = Df = 0$ case with different Pr.

Pr	Elbashbeshy [23]	Chen [24]	Present study
0.72	0.7711	0.76217	0.7622729
1.00	1.0060	1.00616	1.0062684
10.00	7.0921	7.09205	7.0939394

4   Results and discussion

From the numerical computations, dimensionless velocity, temperature and concentration profiles as well as the local skin-friction coefficient, the local Nusselt number and the local Sherwood number are found for the different values of the various physical parameters occurring in the problem. Solutions are obtained for $Pr = 0.71$ (air), $Sc = 0.22$ (hydrogen), $g_s = 10$; $g_c = 5$ (due to free convection problem), while the values of the Dufour number Df and Soret number Sr are taken in such a way that their product has a constant value, let us say $Sr \times Df = 0.06$ (see also Kafoussias and Williams [10], Anghel et al. [11], Postelnicu [12] and El-Aziz [15]) provided that the mean temperature T_m is kept constant. So under the above assumptions our numerical results are shown in Figs. 1–10 and in Table 2.

The effects of suction parameter f_w on the velocity profiles are shown in Fig. 1(a). It is found from this figure that the velocity profiles decrease monotonically with the increase of suction parameter indicating the usual fact that suction stabilizes the boundary layer growth. From this figure it is also seen that for fixed values of f_w, velocity is found to increase and reached a maximum value in a region close to the surface of the stretching sheet, then gradually decreases to zero. The free convection effect is also apparent in this figure. The effect of suction parameter on the temperature and concentration field is displayed in Figs. 1(b) and 1(c) respectively and we see that both the temperature and

concentration decrease with the increase of suction parameter. Suction of the decelerated fluid particles through the porous wall reduces the growth of the hydrodynamic, thermal and concentration boundary layers.

Representative velocity profiles for four typical angles of inclination ($\alpha = 0°, 30°$, $60°$ and $90°$) are presented in Fig. 2(a). It is revealed from Fig. 2(a) that increasing the angle of inclination decreases the velocity. The fact is that as the angle of inclination increases the effect of the buoyancy force due to thermal and mass diffusion decrease by a factor of $\cos \alpha$. Consequently the driving force to the fluid decreases and as a result velocity profiles decrease. From this figure it is also noticeable that the effect of buoyancy force (which is maximum for $\alpha = 0$) overshoots the main stream velocity significantly. From Figs. 2(b)–(c) we also observe that both the thermal and concentration boundary layer thickness increase as the angle of inclination increases.

Figs. 3(a)–(c) represent respectively, the dimensionless velocity, temperature and concentration for various values of the magnetic field parameter M. The presence of a magnetic field normal to the flow in an electrically conducting fluid produces a Lorentz force, which acts against the flow. Thus from this figure we observe that the fluid velocity decreases (for approx. $\eta \leq 2.0$) with the increase of the magnetic field parameter whereas for $\eta \geq 2.0$, the fluid velocity increases with the increase of magnetic parameter. From Fig. 3(b) we see that the temperature profiles increase with the increase of the magnetic field parameter, which implies that the applied magnetic field tends to heat the fluid, and thus reduces the heat transfer from the wall. In Fig. 3(c), the effect of an applied magnetic field is found to increase the concentration profiles.

The effects of the surface heat (or mass) flux exponent parameter r on the dimensionless velocity, temperature and concentration profiles are displayed in Figs. 4(a)–(c) respectively. From Fig. 4(a) it is seen that the velocity profiles decrease with the increasing values of heat (or mass) flux exponent parameter r. Further more from Fig. 4(b) we can see that as r increases, the thermal boundary layer thickness decreases and the temperature gradient at the wall increases. This means a higher value of the heat transfer rate is associated with higher values of r. We also observe from Fig. 4(c) that the concentration profiles decrease as the heat (or mass) flux exponent parameter r increases.

The effects of chemical reaction parameter K on the velocity, temperature as well as concentration distributions are displayed in Figs. 5(a)–(c) respectively. In these figures we have taken the values of $K = -1, 0, 1, 2$. It should be mentioned here that physically positive values of K implies destructive reaction and negative values of K implies generative reaction. It is observed from these figures that an increase in the chemical reaction parameter K leads to the decrease of the velocity and concentration profiles but leads to increase in the temperature profiles. This shows that diffusion rate can be tremendously altered by chemical reaction.

The effects of order of chemical reaction n on the velocity, temperature as well as concentration distributions are displayed in Figs. 6(a)–(c) respectively. It is observed from these figures that an increase in the chemical reaction order n leads to increase the velocity and concentration profiles whereas temperature profiles decrease as n increases.

The influence of Soret number Sr and Dufour number Df on the velocity field are shown in Fig. 7(a). Quantitatively, when $\eta = 1.0$ and Sr decreases from 2.0 to 1.5 (or

Df increases from 0.03 to 0.04), there is 2.18% decrease in the velocity value whereas the corresponding decrease is 1.70% when Sr decreases from 1.0 to 0.5 (or Df increases from 0.06 to 0.12). From Fig. 7(b) when $\eta = 1.0$ and Sr decreases from 2.0 to 1.5 (or Df increases from 0.03 to 0.04), there is 3.66% increase in the temperature, whereas the corresponding increase is 8.33% when Sr decreases from 1.0 to 0.5. In Fig. 7(c) when $\eta = 1.0$ and Sr decreases from 2.0 to 1.5 (or Df increases from 0.03 to 0.04), there is 7.84% decrease in the concentration, whereas the corresponding decrease is 10.18% when Sr decreases from 1.0 to 0.5.

The effects of wall suction parameter fw and variable heat as well as mass fluxes exponent r on the local skin-friction coefficient, the local Nusselt number and the local Sherwood number are shown in Figs. 8(a)–(c) respectively. An increase in the value of r results to a decrease of the local skin-friction coefficient, as shown in Fig. 8(a). Heat transfer results are shown in Fig. 8(b) at selected values of r. Higher heat transfer rates can be obtained by increasing the value of r. Moreover, at a given exponent r, the local Nusselt number is increased as the suction parameter increases. Fig. 8(c) reveals increasing values of r and f_w enhances the mass transfer.

Figs. 9(a)–(c) illustrate the combined effects of magnetic field parameter M and angle of inclination α on the momentum, heat and mass transfer coefficients. In Fig. 9(a), the local skin-friction coefficient is found to decrease due to an increase in the magnetic field strength. This is expected, since the applied magnetic field tends to impede the flow motion and thus to reduce the surface friction force. Also, an increase in the angle of inclination would produce a decrease in the buoyancy force and hence reduce the local skin-friction coefficient. At a given value of α, from Fig. 9(b), it is clear that the presence of the magnetic field gives a reduction of the local Nusselt number in a manner that the local Nusselt number decreases as M increases. This behavior can be readily understood from Fig. 3(b): the temperature gradient at the wall decreases as the magnetic parameter increases, which in turn leads to a reduction in the rate of heat transfer from the surface. It is also noted that the local Nusselt number for $\alpha = 0°$ is larger than that for $\alpha = 60°$, as is expected. The effect of the magnetic field strength on the mass transfer coefficient, in terms of the local Sherwood number, is displayed in Fig. 9(c). It is found that the local Sherwood number decreases with increasing the magnetic field parameter. One can also note from this figure that an increase in the angle of inclination causes a decrease in the Sherwood number.

The effects of chemical reaction parameter K and order of chemical reaction n on the local skin-friction coefficient, the local Nusselt number and the local Sherwood number are shown in Figs. 10(a)–(c) respectively. From these figures we observe that both the local skin-friction coefficient and the local Nusselt number decrease while the local Sherwood number increases as the chemical reaction parameter K increases.

Finally, the effects of the Soret number, Dufour number and the order of the chemical reaction on the local skin-friction coefficient, the local Nusselt number and the local Sherwood number are shown in Table 2. From this table we observe that for fixed values of Sr and Df both the local skin-friction coefficient and the local Nusselt number increase whereas the local Sherwood number decreases as n increases.
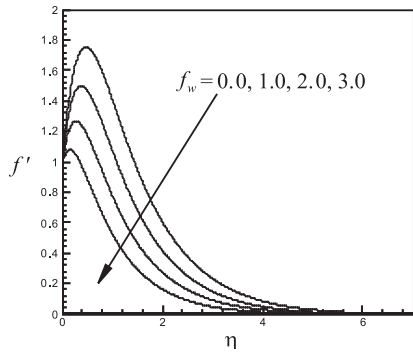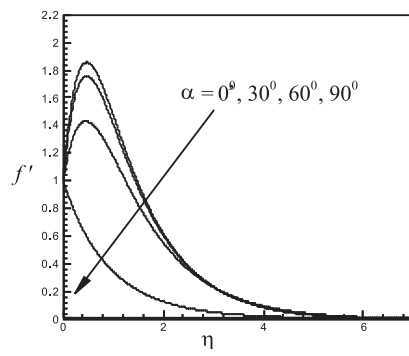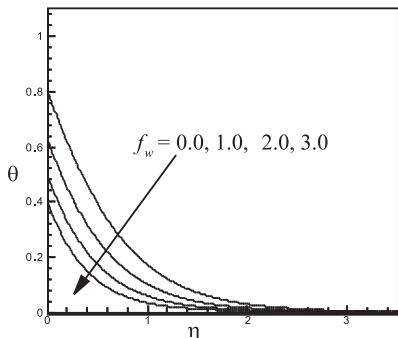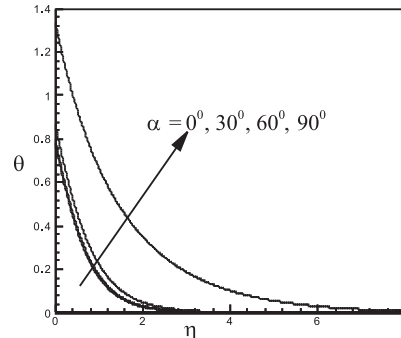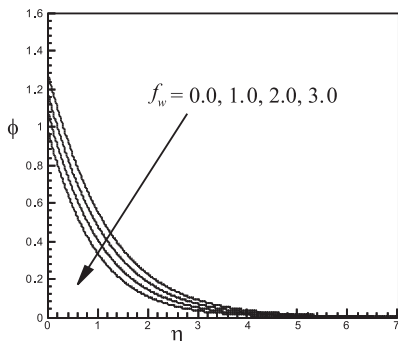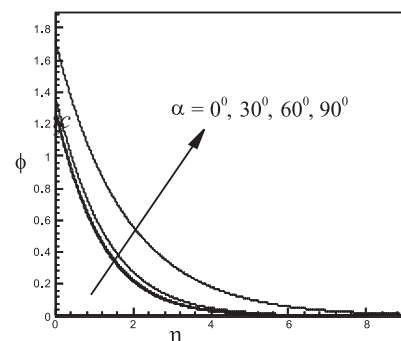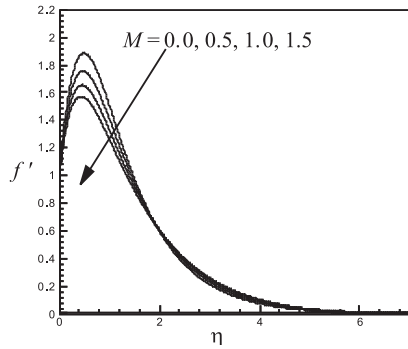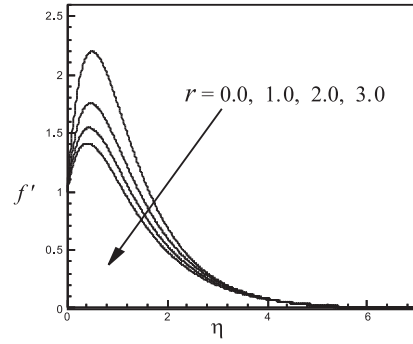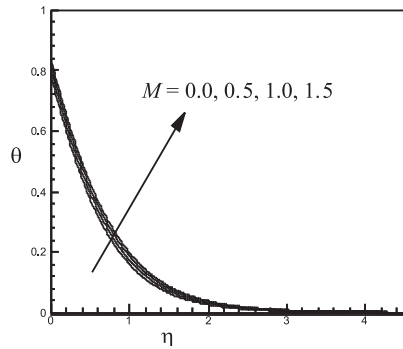
Fig. 1. Variation of dimensionless (a) velocity, (b) temperature and (c) concentration profiles across the boundary layer for different values of fw and for $g_s = 10$, $g_c = 5$, $Pr = 0.71$, $Sc = 0.22$, $r = 1.0$, $M = 0.50$, $K = 1.0$, $n = 1.0$, $Sr = 0.60$, $Df = 0.10$ and $\alpha = 30°$.
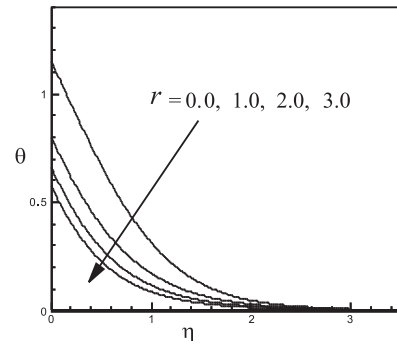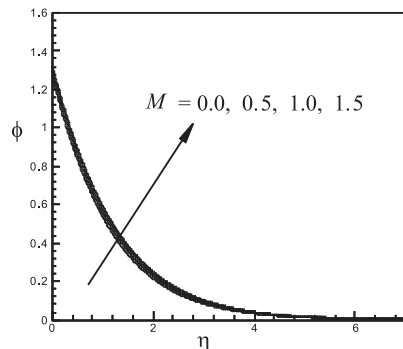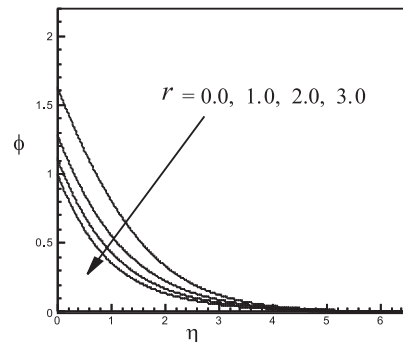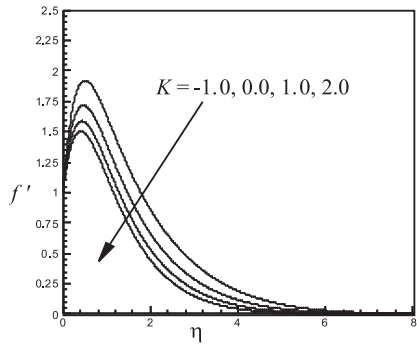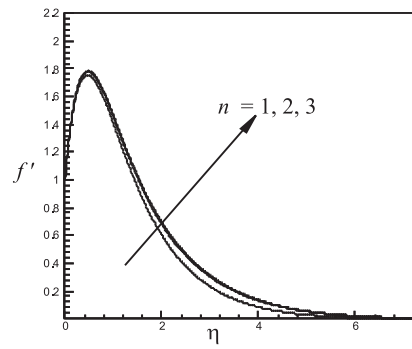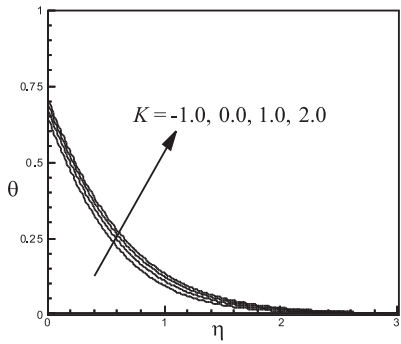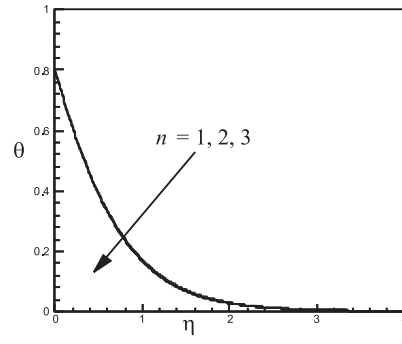
Fig. 2. Variation of dimensionless (a) velocity, (b) temperature and (c) concentration profiles across the boundary layer for different values of α and for $g_s = 10$, $g_c = 5$, $Pr = 0.71$, $Sc = 0.22$, $r = 1.0$, $f_w = 0.5$, $K = 1.0$, $n = 1.0$, $Sr = 0.60$, $Df = 0.10$ and $M = 0.50$.
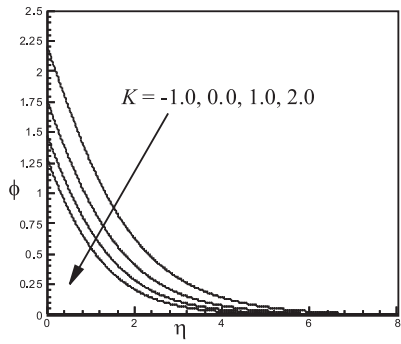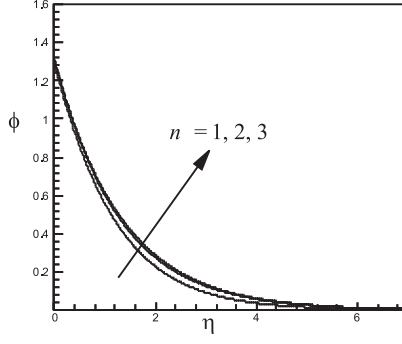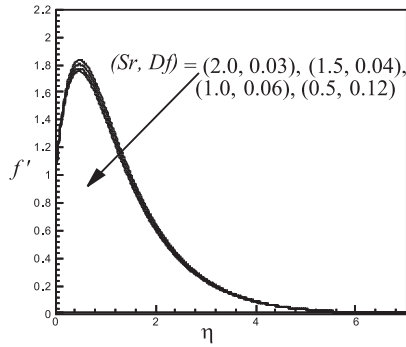
Fig. 3. Variation of dimensionless (a) velocity, (b) temperature and (c) concentration profiles across the boundary layer for different values of M and for $g_s = 10$, $g_c = 5$, $Pr = 0.71$, $Sc = 0.22$, $r = 1.0$, $f_w = 0.50$, $K = 1.0$, $n = 1.0$, $Sr = 0.60$, $Df = 0.10$ and $\alpha = 30°$.
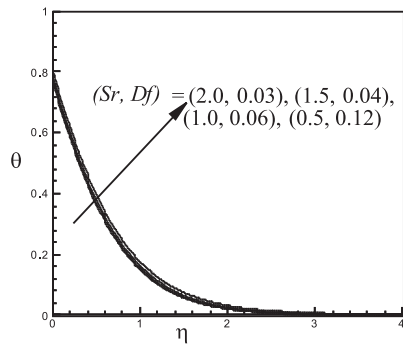
Fig. 4. Variation of dimensionless (a) velocity, (b) temperature and (c) concentration profiles across the boundary layer for different values of r and for $g_s = 10$, $g_c = 5$, $Pr = 0.71$, $Sc = 0.22$, $M = 0.50$, $f_w = 0.5$, $K = 1.0$, $n = 1.0$, $Sr = 0.60$, $Df = 0.10$ and $\alpha = 30°$.
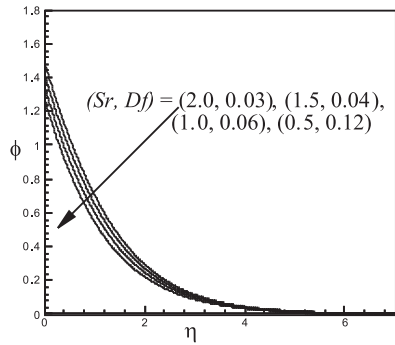
Fig. 5. Variation of dimensionless (a) velocity, (b) temperature and (c) concentration profiles across the boundary layer for different values of K and for $g_s = 10$, $g_c = 5$, $Pr = 0.71$, $Sc = 0.22$, $r = 1.0$, $f_w = 0.50$, $M = 0.50$, $n = 1.0$, $Sr = 0.60$, $Df = 0.10$ and $\alpha = 30°$.

Fig. 6. Variation of dimensionless (a) velocity, (b) temperature and (c) concentration profiles across the boundary layer for different values of n and for $g_s = 10$, $g_c = 5$, $Pr = 0.71$, $Sc = 0.22$, $r = 1.0$, $f_w = 0.50$, $K = 1.0$, $M = 0.50$, $Sr = 0.60$, $Df = 0.10$ and $\alpha = 30°$.
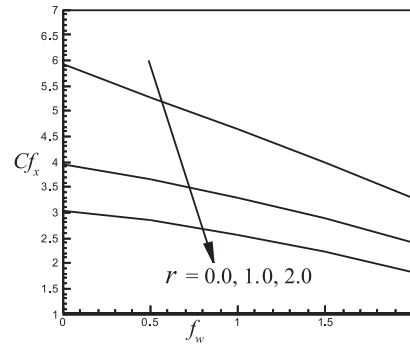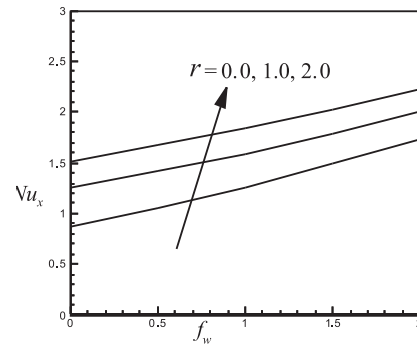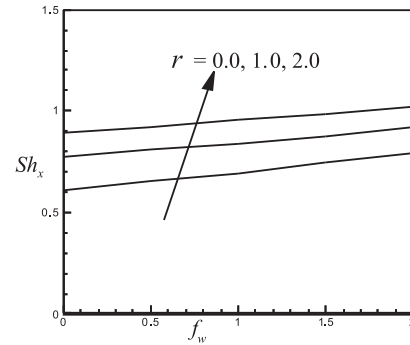
Fig. 7. Variation of dimensionless (a) velocity, (b) temperature and (c) concentration profiles across the boundary layer for different values of (Sr, Df) and for $g_s = 10$, $g_c = 5$, $Pr = 0.71$, $Sc = 0.22$, $r = 1.0$, $f_w = 0.50$, $K = 1.0$, $n = 1.0$, $M = 0.50$ and $\alpha = 30°$.

Fig. 8. Effects of f_w and r on (a) local skin-friction coefficient, (b) local Nusselt number and (c) local Sherwood number, for $g_s = 10$, $g_c = 5$, $Pr = 0.71$, $Sc = 0.22$, $n = 1.0$, $K = 1.0$, $M = 0.50$, $Sr = 0.60$, $Df = 0.10$ and $\alpha = 30°$.

Fig. 9. Effects of α and M on (a) local skin-friction coefficient, (b) local Nusselt number and (c) local Sherwood number, for $g_s = 10$, $g_c = 5$, $Pr = 0.71$, $Sc = 0.22$, $r = 1.0$, $f_w = 0.5$, $K = 1.0$, $n = 1.0$, $Sr = 0.60$ and $Df = 0.10$.

Fig. 10. Effects of n and K on (a) local skin-friction coefficient, (b) local Nusselt number and (c) local Sherwood number, for $g_s = 10$, $g_c = 5$, $Pr = 0.71$, $Sc = 0.22$, $r = 1.0$, $f_w = 0.50$, $M = 0.50$, $Sr = 0.60$, $Df = 0.10$ and $\alpha = 30°$.
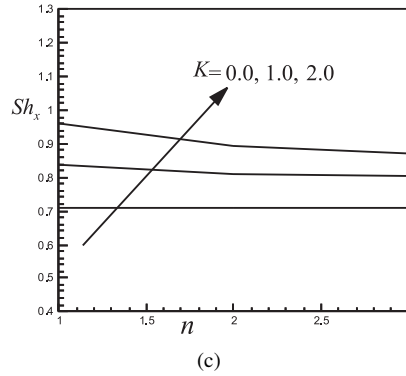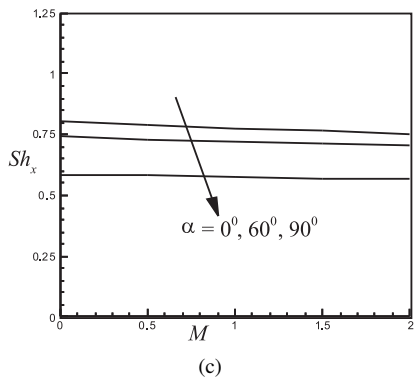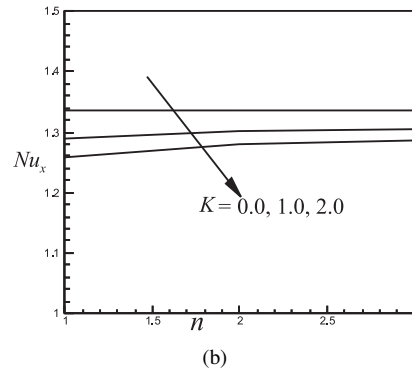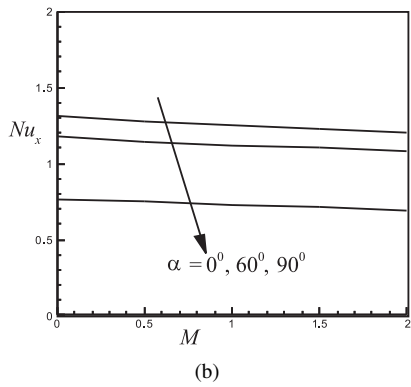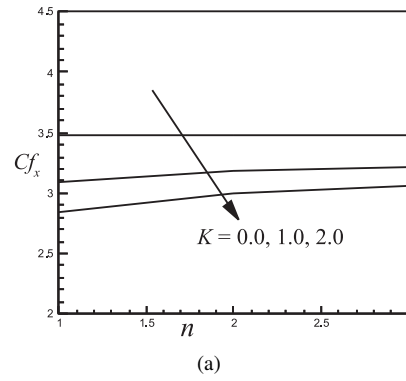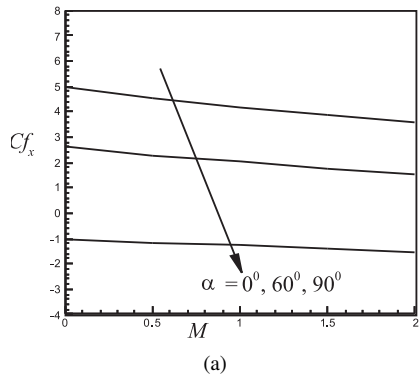
Table 2. Effects of Sr, Df and n on the local skin-friction coefficient (Cf_x), local Nusselt number (Nu_x) and local Sherwood number (Sh_x) for $g_s = 10$, $g_c = 5$, $Pr = 0.71$, $Sc = 0.22$, $r = 1.0$, $f_w = 0.50$, $K = 1.0$, $M = 0.50$ and $\alpha = 30°$.

n	Sr	Df	Cf_x	Nu_x	Sh_x
1	2.0	0.03	3.3565689	1.4361584	0.6767115
2	2.0	0.03	3.3781935	1.4429034	0.6757279
3	2.0	0.03	3.3953886	1.4432882	0.6750276
1	1.0	0.06	3.1145821	1.4024461	0.7542388
2	1.0	0.06	3.1893935	1.4121446	0.7414636
3	1.0	0.06	3.2014252	1.4140062	0.7404342
1	0.5	0.12	3.0271220	1.3662225	0.8023145
2	0.5	0.12	3.1162475	1.3770869	0.7805707
3	0.5	0.12	3.1402625	1.3796087	0.7766252

5   Conclusions

In this paper we have studied numerically the effects of variable chemical reaction and variable electric conductivity on free convection and mass transfer flow of a viscous, incompressible and electrically conducting fluid over an inclined stretching sheet with variable heat and mass fluxes under the influence of Dufour and Soret effects. From the present numerical investigations we see that the velocity profiles decrease with the increasing values of magnetic field parameter, suction parameter, angle of inclination to the vertical, heat (or mass) flux parameter and chemical reaction parameter whereas it increases with increasing value of order of chemical reaction. The temperature profiles increase with the increasing values of magnetic field parameter, angle of inclination to the vertical, heat (or mass) flux parameter as well as chemical reaction parameter whereas it decreases with increasing values of the suction parameter, order of chemical reaction and heat (or mass) flux exponent. The concentration profile increases with an increasing value of magnetic field parameter, angle of inclination to the vertical direction and order of chemical reaction whereas it decreases with the increasing values of the suction parameter, heat (or mass) flux exponent as well as chemical reaction parameter. The numerical results show that higher order heat and mass fluxes index has more decreasing effect on the hydrodynamic, thermal and concentration boundary layers compared to the zero order (constant heat and mass fluxes) indexes. The presented analysis has also shown that the flow field is appreciably influenced by the Soret and Dufour effects. Therefore, we can say that for fluids with medium molecular weight (H_2, air), Dufour and Soret effects should not be neglected.

Acknowledgements

References

1. H.I. Andersson, O.R. Hansen, B. Holmedal, Diffusion of a chemically reactive species from a stretching sheet, *Int. J. Heat Mass Transfer*, **37**, pp. 465–474, 1994.

2. S.P. Anjalidevi, R. Kandasamy, Effects of chemical reaction heat and mass transfer on laminar flow along a semi-infinite horizontal plate, *Heat Mass Transfer*, **35**, pp. 465–467, 1999.

3. H.S. Takhar, A.J. Chamkha G. Nath, Flow and mass transfer on a stretching sheet with a magnetic field and chemically reactive species, *Int. J. Eng. Sci.*, **38**, pp. 1303–1310, 2000.

4. A. Afify, MHD free convective flow and mass transfer over a stretching sheet with chemical reaction, *Heat Mass Transfer*, **40**, pp. 495–500, 2004.

5. E.M. Abo-Eldahab, A.M. Salem, MHD flow and heat transfer of non-Newtonian power-law fluid with diffusion and chemical reaction on a moving cylinder, *Heat Mass Transfer*, **41**, pp. 703–708, 2005.

6. M.S. Alam, M.M. Rahman, M.A. Sattar, Effects of chemical reaction and thermophoresis on MHD mixed convective heat and mass transfer flow along an inclined plate in the presence of heat generation/absorption with viscous dissipation and joule heating, *Can. J. Phys.*, **86**, pp. 1057–1066, 2008.

7. M.S. Alam, M.M. Rahman, M.A. Sattar, Transient magnetohydrodynamic free convective heat and mass transfer flow with thermophoresis past a radiate inclined permeable plate in the presence of variable chemical reaction and temperature dependent viscosity, *Nonlinear Anal. Model. Control*, **14**(1), pp. 3–20, 2009.

8. Bergaman, T. L. and Srinivasan, R., Numerical solution of Soret indused double diffusive in an initially uniform concentration binary liquid, *Int. J. Heat Mass Transfer*, **32**(4), pp. 679–687, 1989.

9. G. Zimmerman, U. Muller, C. Benard, Convection in a two component system with Soret effect, *Int. J. Heat Mass Transfer*, **35**(9), pp. 2245–2256, 1992.

10. N.G. Kafoussias, E.W. Williams, Thermal-diffusion and diffusion-thermo effects on mixed free-forced convective and mass transfer boundary layer flow with temperature dependent viscosity, *Int. J. Eng. Sci.*, **33**(9), pp. 1369–1384, 1995.

11. M. Anghel, H.S. Takhar, I. Pop, Dufour and Soret effects on free convection boundary layer over a vertical surface embedded in a porous medium, *Stud. Univ. Babes-Bolyai, Math.*, **45**, pp. 11–21, 2000.

12. A. Postelnicu, Influence of a magnetic field on heat and mass transfer by natural convection from vertical surfaces in porous media considering Soret and Dufour effects, *Int. J. Heat Mass Transfer*, **47**, pp. 1467–1472, 2004.

13. M.S. Alam, M.M. Rahman, M.A. Maleque, M. Ferdows, Dufour and Soret effects on steady MHD combined free-forced convective and mass transfer flow past a semi-infinite vertical plate, *Thammasat Int. J. Sci. Technol.*, **11**(2), pp. 1–12, 2006.

14. A.J. Chamkha, A. Ben-Nakhi, MHD Mixed convection-radiation interaction along a permeable surface immersed in a porous medium in the presence of Soret and Dufour's Effects, *Heat Mass Transfer*, **44**, pp. 845–856, 2008.

15. M.A. El-Aziz, Thermal-diffusion and diffusion-thermo effects on combined heat and mass transfer by hydromagnetic three-dimensional free convection over a permeable stretching surface with radiation, *Phys. Lett. A*, **372**, pp. 263–272, 2008.

16. A.A. Afify, Similarity solution in MHD: Effects of thermal diffusion and diffusion thermo on free convective heat and mass transfer over a stretching surface considering suction or injection, *Commun. Nonlinear Sci. Numer. Simul.*, **14**, pp. 2202–2214, 2009.

17. O. Anwar Bég, A.Y. Bakier, V.R. Prasad, Numerical study of free convection magneto-hydrodynamic heat and mass transfer from a stretching surface to a saturated porous medium with Soret and Dufour effects, *Comput. Mater. Sci.*, **46**, pp. 57–65, 2009.

18. T. Hayat, M. Mustafa, I. Pop, Heat and mass transfer for Soret and Dufour's effect on mixed convection boundary layer flow over a stretching vertical surface in a porous medium filled with a viscoelastic fluid, *Commun. Nonlinear Sci. Numer. Simul.*, **15**, pp. 1183–1196, 2010.

19. K.A. Helmy, MHD boundary layer equations for power law fluids with variable electric conductivity, *Mechanica*, **30**, pp. 187–200, 1995.

20. M. Acharya, L.P. Singh, G.C. Dash, Heat and mass transfer over an accelerating surface with heat source in the presence of suction and blowing, *Int. J. Eng. Sci.*, **37**, pp. 189–211, 1999.

21. P.R. Nachtsheim, P. Swigert, Satisfaction of the asymptotic boundary conditions in numerical solution of the system of non-linear equations of boundary layer type, NASA TND-3004, 1965.

22. M.S. Alam, M.M. Rahman, M.A. Samad, Numerical study of the combined free-forced convection and mass transfer flow past a vertical porous plate in a porous medium with heat generation and thermal diffusion, *Nonlinear Anal. Model. Control*, **11**(4), pp. 331–343, 2006.

23. E.M.A. Elbashbeshy, Heat transfer over a stretching surface with variable surface heat flux, *J. Phys. D, Appl. Phys.*, **31**, pp. 1951–1954, 1998.

24. C.H. Chen, Effects of magnetic field and suction/injection on convection heat transfer of non-Newtonian power-law fluids past a power-law stretched sheet with surface heat flux, *Int. J. Therm. Sci.*, **47**(7), pp. 954–961, 2008.